

# Study of $\chi_b$ production at $\sqrt{s} = 7$ and 8 TeV

I. Belyaev<sup>1,2</sup>, C. Bozzi<sup>3</sup>, H. Dijkstra<sup>1</sup>, A. Mazurov<sup>1,4</sup>.

<sup>1</sup>*CERN*, <sup>2</sup>*ITEP, Moscow*, <sup>3</sup>*INFN Sezione di Ferrara*, <sup>4</sup>*Università di Ferrara*

## Abstract

A study of  $\chi_b$  production at LHCb is performed on data collected during 2011 and 2012, by reconstructing  $\chi_b(1P, 2P, 3P) \rightarrow \Upsilon(1S)\gamma$  decays. The differential production cross sections, relative to the  $\Upsilon(1S)$ , are measured as a function of  $\Upsilon(1S)$  transverse momentum and rapidity. The  $\chi_b \rightarrow \Upsilon(2S)\gamma$  and  $\chi_b \rightarrow \Upsilon(3S)\gamma$  decays are also investigated. The  $\chi_b(3P)$  mass is measured.



# 1 Introduction

It is expected that a significant fraction of the production cross-section of  $J/\psi$  and  $\Upsilon$  states in hadron collisions is due to feed-down from heavier quarkonium states. A study of this effect is important for the interpretation of onia production cross section and polarization measurements in hadron collisions. For P-wave quarkonia, measurements of  $\chi_c$  have been reported by CDF [?], HERA-B [?] and LHCb [?], whereas CDF [?] and ATLAS [?] have performed measurements involving  $\chi_b$  states. LHCb has reported [?] a preliminary measurement of the  $\chi_b$  production cross-section, and subsequent decay into  $\Upsilon(1S) \gamma$ , relative to the  $\Upsilon(1S)$  production. This measurement was performed on 2011 data, in a region defined by  $6 \text{ GeV}/c < p_T(\Upsilon(1S)) < 15 \text{ GeV}/c$  and  $2.0 < y < 4.5$ .

This note presents an update of the previous LHCb study. Data collected in 2012 were also analyzed, allowing for cross-section measurements at  $\sqrt{s} = 8 \text{ TeV}$ . Using the full integrated luminosity allows for a measurement of the differential cross-section in  $p_T$  and rapidity bins of the  $\Upsilon(1S)$ , and to study the production of  $\chi_b(2P)$  And  $\chi_b(3P)$ . A measurement of the  $\chi_b(3P)$  mass is also performed by combining data collected in 2011 and 2012.

The analysis proceeds through the reconstruction of  $\Upsilon(nS)$  candidates via their dimuon decays, and their subsequent pairing with a photon to look for  $\chi_b(mP) \rightarrow \Upsilon(nS)\gamma$  decays. Ratios of  $\chi_b(mP)$  to  $\Upsilon(nS)$  production cross section can be written as

$$\frac{\sigma(pp \rightarrow \chi_b(mP) \rightarrow \Upsilon(nS)\gamma)}{\sigma(pp \rightarrow \Upsilon(nS))} = \frac{N_{\chi_b(mP) \rightarrow \Upsilon(nS)\gamma}}{N_{\Upsilon(nS)}} \times \frac{\epsilon_{\Upsilon(nS)}}{\epsilon_{\chi_b(mP) \rightarrow \Upsilon(nS)\gamma}} = \frac{N_{\chi_b(mP) \rightarrow \Upsilon(nS)\gamma}}{N_{\Upsilon(nS)}} \times \frac{1}{\epsilon_{\gamma}^{eco}} \quad (1)$$

where  $N_{\Upsilon(nS)}$  and  $N_{\chi_b(mP) \rightarrow \Upsilon(nS)\gamma}$  are the  $\Upsilon(nS)$  and  $\chi_b(mP)$  yields,  $\epsilon_{\Upsilon(nS)}$  and  $\epsilon_{\chi_b(mP) \rightarrow \Upsilon(nS)\gamma}$  are their corresponding selection efficiencies. The latter are the product of geometric acceptance, trigger efficiency and reconstruction efficiency. Since the selection criteria for the two samples differ only in the reconstruction of a photon, the efficiency ratio can be replaced by  $1/\epsilon_{\gamma}$ , the reconstruction efficiency for the photon from the  $\chi_b$  decay. Similar expressions may be used to compute differential cross sections in  $\Upsilon$   $p_T$  and rapidity bins.

## 2 Data and Monte-Carlo samples

The data sample used in this analysis has been collected by LHCb in 2011 and 2012, at center-of-mass energies of  $\sqrt{s} = 7 \text{ TeV}$  and  $8 \text{ TeV}$ , respectively. For 2011, both Reco12 (?) and Reco14/Stripping 20 samples were used. The former was privately stripped by Vanya (?).

The corresponding integrated luminosities are...

Events are triggered by...

and subsequently stripped by StrippingMicroDSTDiMuonDiMuonIncLine. This line takes StdLooseDiMuon as input, applies requirements on muon momentum, transverse

36 momentum, track and vertex chisquares, and transverse momentum of the composite  
37 particle  
38 `(MINTREE('mu+'==ABSID,PT) > 650.0 *MeV) & (MINTREE('mu+'==ABSID,P)`  
39 `> -8000.0 *MeV) & (MAXTREE('mu+'==ABSID,TRCHI2DOF) < 5.0) & (in_range(`  
40 `3000.0 *MeV, MM, 100000000.0 *MeV)) & (VFASPF(VCHI2PDOF)< 20.0) & (PT >`  
41 `2000.0)`  
42 and saves the output in MicroDST format. The StdLooseDiMuon list contains pairs of  
43 oppositely charged muon from the StdAllLooseMuons list with the additional requirement  
44 CombinationCut (ADOCACHI2CUT(30, ")), MotherCut (VFASPF(VCHI2) ; 25)  
45 Simulated data were produced with 2011 conditions. Six samples of XX million events  
46 each were generated, each corresponding to a different decay under study. Table ??  
47 summarizes the various samples used in this analysis.

### 48 **3 Event Selection criteria**

49 Pairs of opposite charge tracks are used to form  $\Upsilon$  candidates. Both tracks are identified  
50 as muons and must originate from a common vertex Put selection criteria here, discuss  
51 discriminating variables, put all cuts in a table.

### 52 **4 Data - Monte Carlo comparison**

53 A comparison of the distribution of the relevant observables used in this analysis was  
54 performed on real and simulated data, in order to assess the reliability of Monte Carlo in  
55 computing efficiencies. It should be stressed that, since a relative branching fraction is  
56 measured, systematic effects cancel at first order.

57 Combinatorial background has been subtracted in real data by using an *sPlot* technique,  
58 where the discriminant distribution is... The resulting signal weights are used to obtain  
59 the signal distribution for each relevant variable. These distributions are then compared  
60 with simulation, as shown in Figures ??-??. The agreement is generally very good, giving  
61 confidence that the Monte Carlo describes correctly the decays under study.

### 62 **5 Determination of $\Upsilon$ yields**

63 The yields of  $\Upsilon(1S)$ ,  $\Upsilon(2S)$  and  $\Upsilon(3S)$  particles are determined by fitting the dimuon  
64 invariant mass distribution. The combinatorial background is described by... The  $\Upsilon$  peaks  
65 are parameterized with... The  $\alpha$  and  $n$  parameters of the Crystal Ball function are fixed  
66 to... etc... the floating parameters in the fit are... Figure XX and YY show the invariant  
67 mass distribution in 2011 and 2012 data, respectively. The event yields and other fit  
68 parameters are reported in Table ZZ. The systematic uncertainties in the  $\Upsilon$  yields are  
69 determined by... They are discussed in ??.

Table 1: The order of background polynom  $n$

$p_T^{\Upsilon(1S)}$ interval	Polynom order
10 — 12 GeV/c	5
12 — 18 GeV/c	3
18 — 30 GeV/c	2

## 6 Determination of the $\chi_b$ yields

The yields of  $\chi_b(1P, 2P, 3P) \rightarrow \Upsilon(1S) \gamma$  are determined with fits to the  $m(\mu^+ \mu^- \gamma) - m(\mu^+ \mu^-)$  invariant mass difference. Combinatorial background is described by exponential function multiplied by polynom (Eq):

$$e^{-\tau x} (a_1 x + a_2 x^2 + \dots + a_n x^n) \quad (2)$$

The order of polynom  $n$  depends on  $p_T^{\Upsilon(1S)}$  interval as shown in table ??  
 ..., signal are parametrized with ... Mention how you fix and float the various parameters of this fit... Figure XX and Table YY show the results...

## 7 Determination of selection efficiencies

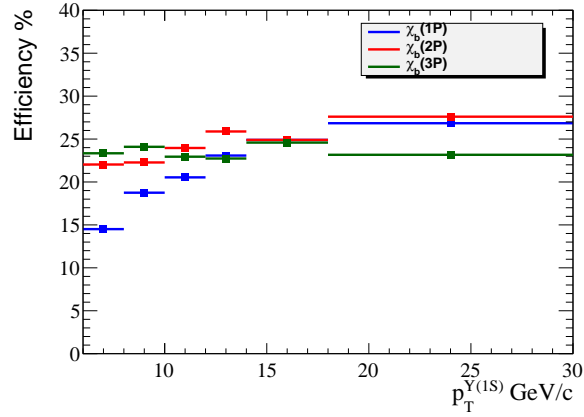


Figure 1: Monte-Carlo data. Fraction of  $\Upsilon(1S)$  originating from  $\chi_b$  decays for different  $p_T^{\Upsilon(1S)}$  intervals.

## 78 8 Determination of the $\chi_b$ production cross section

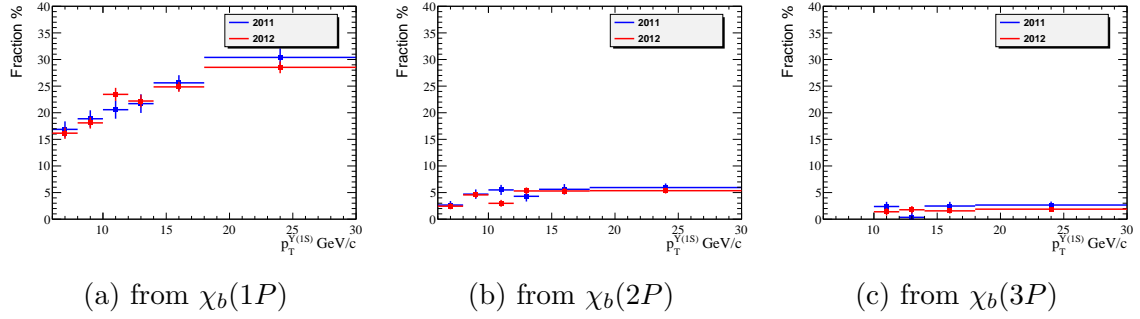


Figure 2: Fraction of  $\Upsilon(1S)$  originating from  $\chi_b$  decays for different  $p_T^{\Upsilon(1S)}$  intervals.

## 79 9 Systematic Uncertainties

## 80 10 Determination of the $\chi_b$ masses

## 81 11 Conclusion

Table 2: Summary of fraction determination.

$\Upsilon(1S)$ transverse momentum interval in GeV/c								
	6 - 8	8 - 10	10 - 12	12 - 14	14 - 16	16 - 18	14 - 18	18 - 30
Parameters obtained by counting MC matched events for $\chi_{b1}(1P)$ decay								
$N_{\chi_{b1}(1P)}^{MC}$	6142	5262	3583	2217	1286	798	2081	1092
$N_{\Upsilon(1S)}^{MC}$	41,738	27,845	16,756	9452	5164	2913	8077	3852
$\varepsilon_{\chi_{b1}(1P)}^{MC} \%$	14.7	18.9	21.4	23.5	24.9	27.4	25.8	28.3
Parameters obtained by counting MC matched events for $\chi_{b2}(1P)$ decay								
$N_{\chi_{b2}(1P)}^{MC}$	4303	2659	1272	629	312	147	458	152
$N_{\Upsilon(1S)}^{MC}$	29,145	14,021	6475	2800	1305	610	1915	635
$\varepsilon_{\chi_{b2}(1P)}^{MC} \%$	14.8	19.0	19.6	22.5	23.9	24.1	23.9	23.9
Parameters obtained by counting MC matched events for $\chi_{b1}(2P)$ decay								
$N_{\chi_{b1}(2P)}^{MC}$	4551	3197	2002	1123	649	335	984	500
$N_{\Upsilon(1S)}^{MC}$	19,711	13,545	8034	4337	2533	1368	3901	1865
$\varepsilon_{\chi_{b1}(2P)}^{MC} \%$	23.1	23.6	24.9	25.9	25.6	24.5	25.2	26.8
Parameters obtained by counting MC matched events for $\chi_{b2}(2P)$ decay								
$N_{\chi_{b2}(2P)}^{MC}$	3658	1659	823	418	171	94	264	105
$N_{\Upsilon(1S)}^{MC}$	17,358	8023	3607	1642	773	329	1102	379
$\varepsilon_{\chi_{b2}(2P)}^{MC} \%$	21.1	20.7	22.8	25.5	22.1	28.6	24.0	27.7
Parameters obtained by counting MC matched events for $\chi_{b1}(3P)$ decay								
$N_{\chi_{b1}(3P)}^{MC}$	4568	3070	1733	1041	556	308	864	403
$N_{\Upsilon(1S)}^{MC}$	18,105	12,120	7145	4101	2248	1267	3515	1621
$\varepsilon_{\chi_{b1}(3P)}^{MC} \%$	25.2	25.3	24.3	25.4	24.7	24.3	24.6	24.9
Parameters obtained by counting MC matched events for $\chi_{b2}(3P)$ decay								
$N_{\chi_{b2}(3P)}^{MC}$	2555	1241	508	216	129	58	184	48
$N_{\Upsilon(1S)}^{MC}$	11,754	5471	2365	1099	516	255	771	228
$\varepsilon_{\chi_{b2}(3P)}^{MC} \%$	21.7	22.7	21.5	19.7	25.0	22.7	23.9	21.1
Average MC efficiency of $\chi_{b1}$ and $\chi_{b2}$ MeV/c <sup>2</sup> in %								
$\varepsilon_{\chi_{b1}(1P)}^{MC}$	14.7	18.9	20.5	23.0	24.4	25.7	24.8	26.1
$\varepsilon_{\chi_{b1}(2P)}^{MC}$	22.1	22.1	23.9	25.7	23.9	26.5	24.6	27.3
$\varepsilon_{\chi_{b1}(3P)}^{MC}$	23.5	24.0	22.9	22.5	24.9	23.5	24.2	23.0
Parameters obtained by fitting MC distributions in MeV/c <sup>2</sup>								
$\Delta m_{\chi_{b1}(1P)}$	428.18 $\pm$ 0.34	427.5 $\pm$ 0.4	427.3 $\pm$ 0.4	427.2 $\pm$ 0.5	427.1 $\pm$ 0.6	428.1 $\pm$ 0.8	427.4 $\pm$ 0.5	428.0 $\pm$ 0.6
$\Delta m_{\chi_{b2}(1P)}$	448.2 $\pm$ 0.5	447.2 $\pm$ 0.6	447.3 $\pm$ 0.7	447.0 $\pm$ 0.9	446.7 $\pm$ 1.4	444.0 $\pm$ 1.9	446.1 $\pm$ 1.1	446.1 $\pm$ 1.4
$\Delta m_{\chi_{b1}(2P)}$	786.4 $\pm$ 0.6	786.5 $\pm$ 0.7	786.7 $\pm$ 0.9	786.5 $\pm$ 1.0	788.8 $\pm$ 1.3	788.7 $\pm$ 1.6	789.0 $\pm$ 1.0	790.2 $\pm$ 1.3
$\Delta m_{\chi_{b2}(2P)}$	800.8 $\pm$ 0.7	800.9 $\pm$ 1.0	799.5 $\pm$ 1.2	802.5 $\pm$ 1.7	798.3 $\pm$ 2.3	804 $\pm$ 4	799.9 $\pm$ 1.9	802.8 $\pm$ 3.2
$\Delta m_{\chi_{b1}(3P)}$	1046.2 $\pm$ 0.7	1046.8 $\pm$ 0.8	1047.9 $\pm$ 1.0	1047.4 $\pm$ 1.3	1048.4 $\pm$ 1.7	1051.1 $\pm$ 2.2	1049.5 $\pm$ 1.3	1050.9 $\pm$ 1.9
$\Delta m_{\chi_{b2}(3P)}$	1058.0 $\pm$ 1.0	1055.9 $\pm$ 1.2	1058.1 $\pm$ 2.1	1059.6 $\pm$ 2.8	1064 $\pm$ 4	1062 $\pm$ 5	1063.9 $\pm$ 2.8	1061 $\pm$ 7
$\sigma_{\chi_{b1}(1P)}$	23.14 $\pm$ 0.35	22.3 $\pm$ 0.4	21.1 $\pm$ 0.4	19.9 $\pm$ 0.5	19.3 $\pm$ 0.6	19.7 $\pm$ 0.8	19.4 $\pm$ 0.5	19.0 $\pm$ 0.6
$\sigma_{\chi_{b2}(1P)}$	24.2 $\pm$ 0.5	23.3 $\pm$ 0.6	21.4 $\pm$ 0.7	20.7 $\pm$ 1.0	20.9 $\pm$ 1.3	23.5 $\pm$ 1.5	22.4 $\pm$ 0.9	15.8 $\pm$ 1.3
$\sigma_{\chi_{b1}(2P)}$	34.2 $\pm$ 0.8	33.5 $\pm$ 0.8	32.9 $\pm$ 1.0	32.3 $\pm$ 0.8	33.2 $\pm$ 1.0	29.4 $\pm$ 1.2	30.7 $\pm$ 0.8	29.2 $\pm$ 1.2
$\sigma_{\chi_{b2}(2P)}$	37.5 $\pm$ 0.7	33.5 $\pm$ 1.1	32.6 $\pm$ 1.0	33.1 $\pm$ 1.5	30.6 $\pm$ 1.8	36.1 $\pm$ 2.9	31.6 $\pm$ 1.5	32.1 $\pm$ 2.6
$\sigma_{\chi_{b1}(3P)}$	47.2 $\pm$ 0.6	45.9 $\pm$ 0.7	43.4 $\pm$ 0.9	43.3 $\pm$ 1.1	43.7 $\pm$ 1.3	41.6 $\pm$ 1.7	42.3 $\pm$ 1.0	40.2 $\pm$ 1.5
$\sigma_{\chi_{b2}(3P)}$	49.0 $\pm$ 0.9	42.0 $\pm$ 1.2	43.1 $\pm$ 2.1	40.2 $\pm$ 3.0	45.3 $\pm$ 2.9	40 $\pm$ 4	38.1 $\pm$ 2.4	41 $\pm$ 6

## 82 Appendices

## 83 A Fitting parameters summary

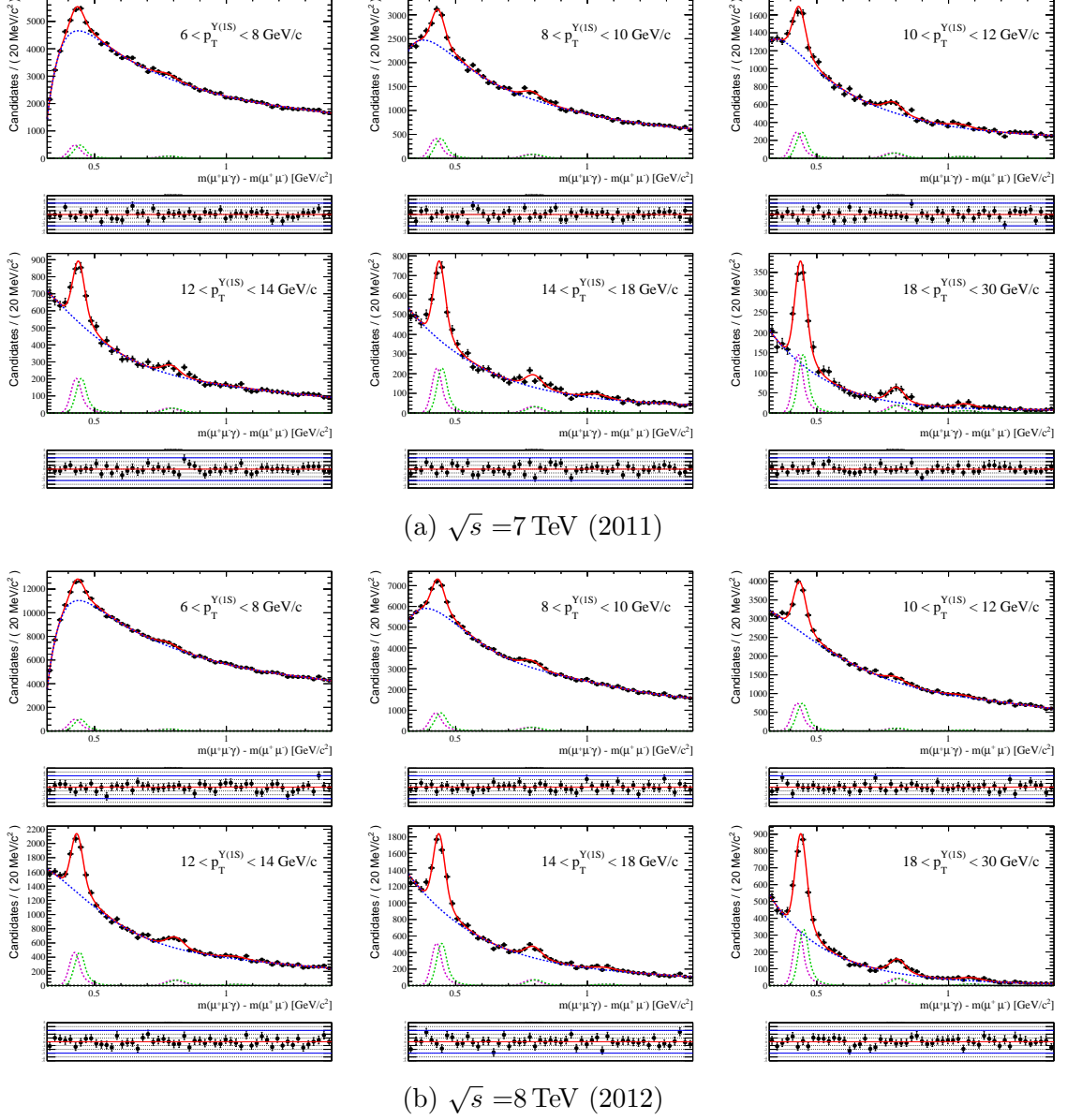


Figure 3: Mass difference of the  $\mu^+\mu^-\gamma$  system and  $\mu^+\mu^-$  system for the data for specified interval of transverse momentum of the  $Y(1S)$ . The red solid line is the result of the fit described in the text. Blue dashed line is the background contribution obtained from the fit. Magenta and green dashed lines are  $\chi_{b1}$  and  $\chi_{b2}$  signal contribution obtained from the fit.



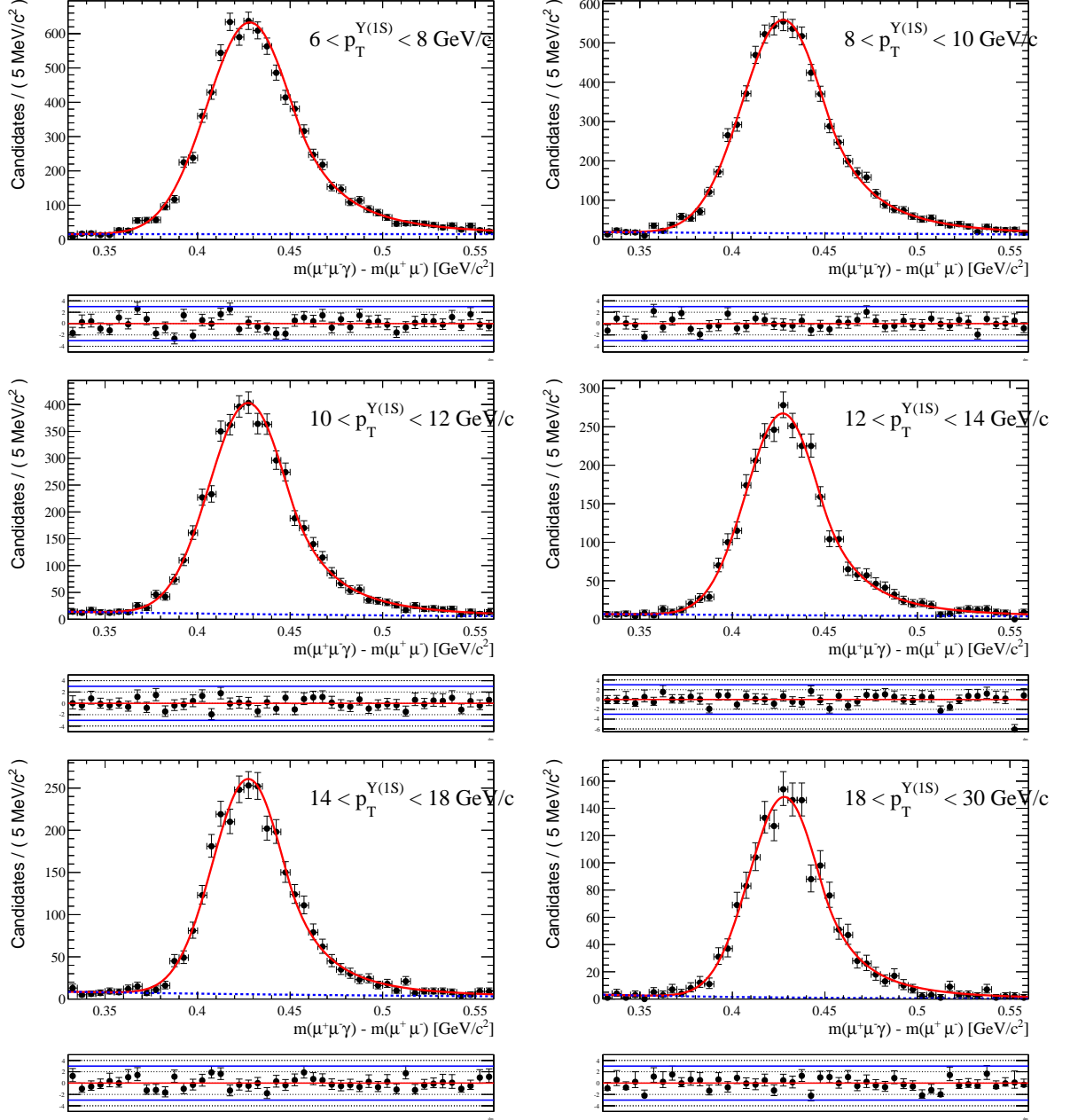


Figure 4:  $\chi_{b1}(1P)$

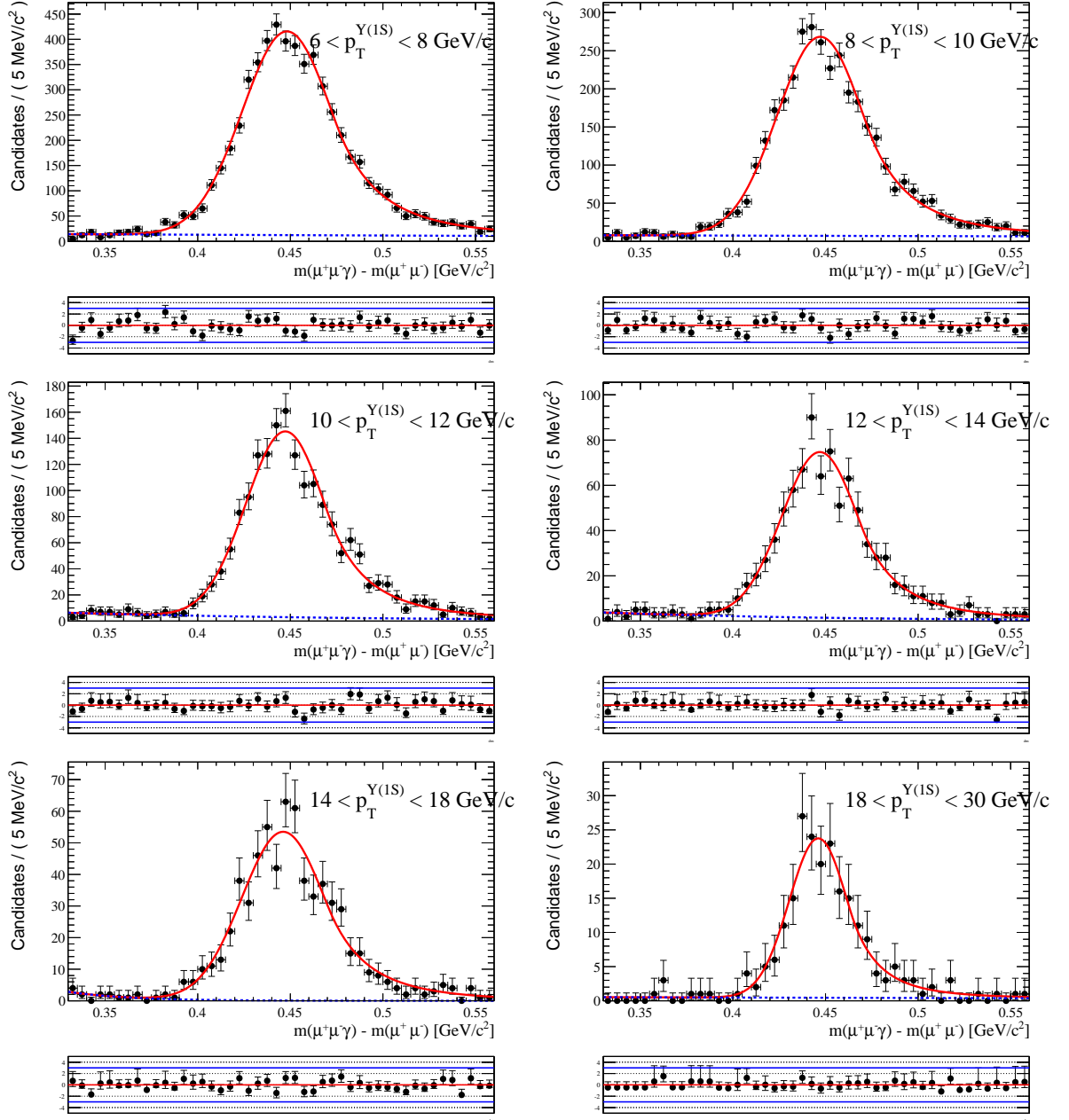


Figure 5:  $\chi_{b2}(1P)$

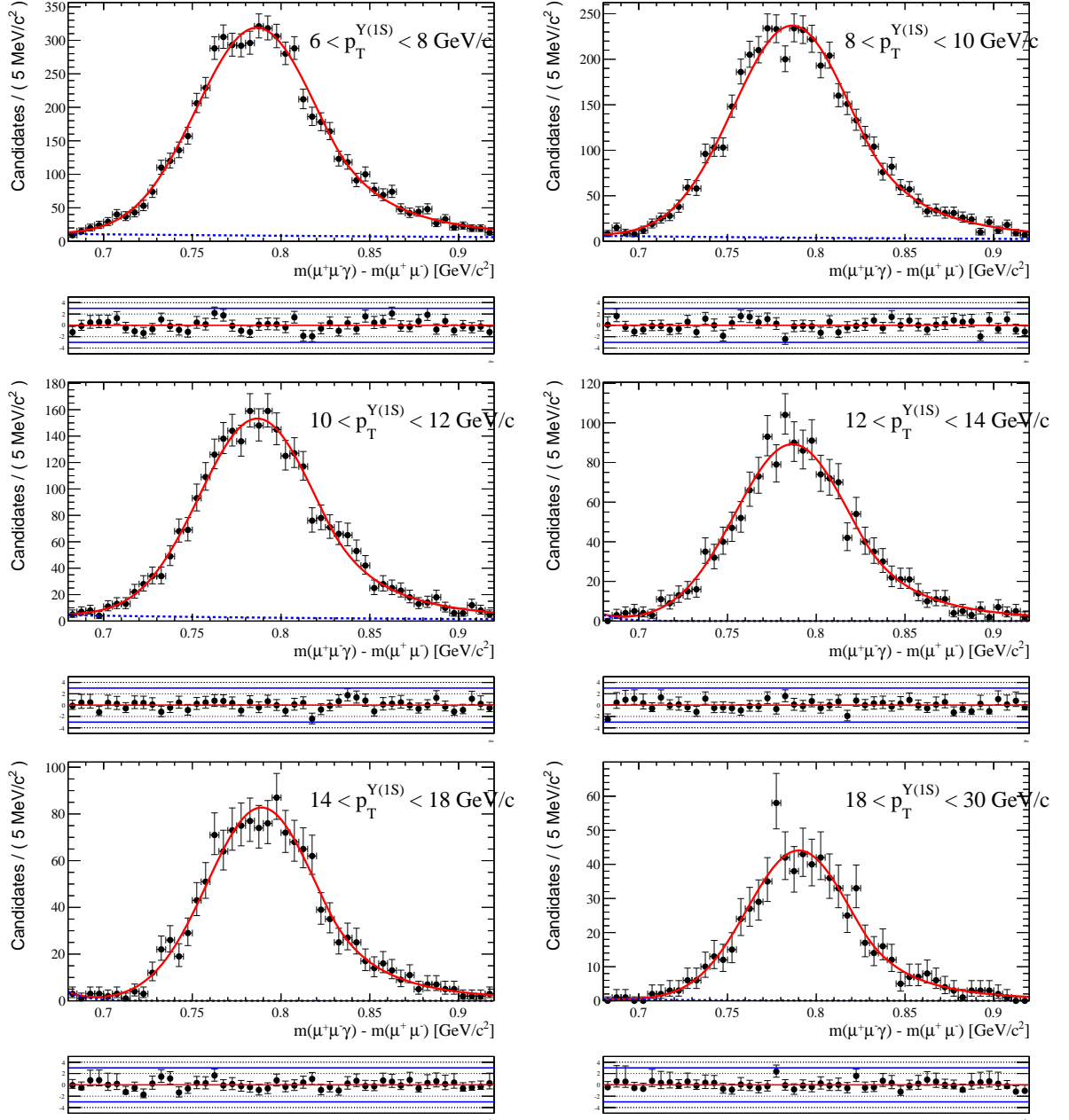


Figure 6:  $\chi_{b1}(2P)$

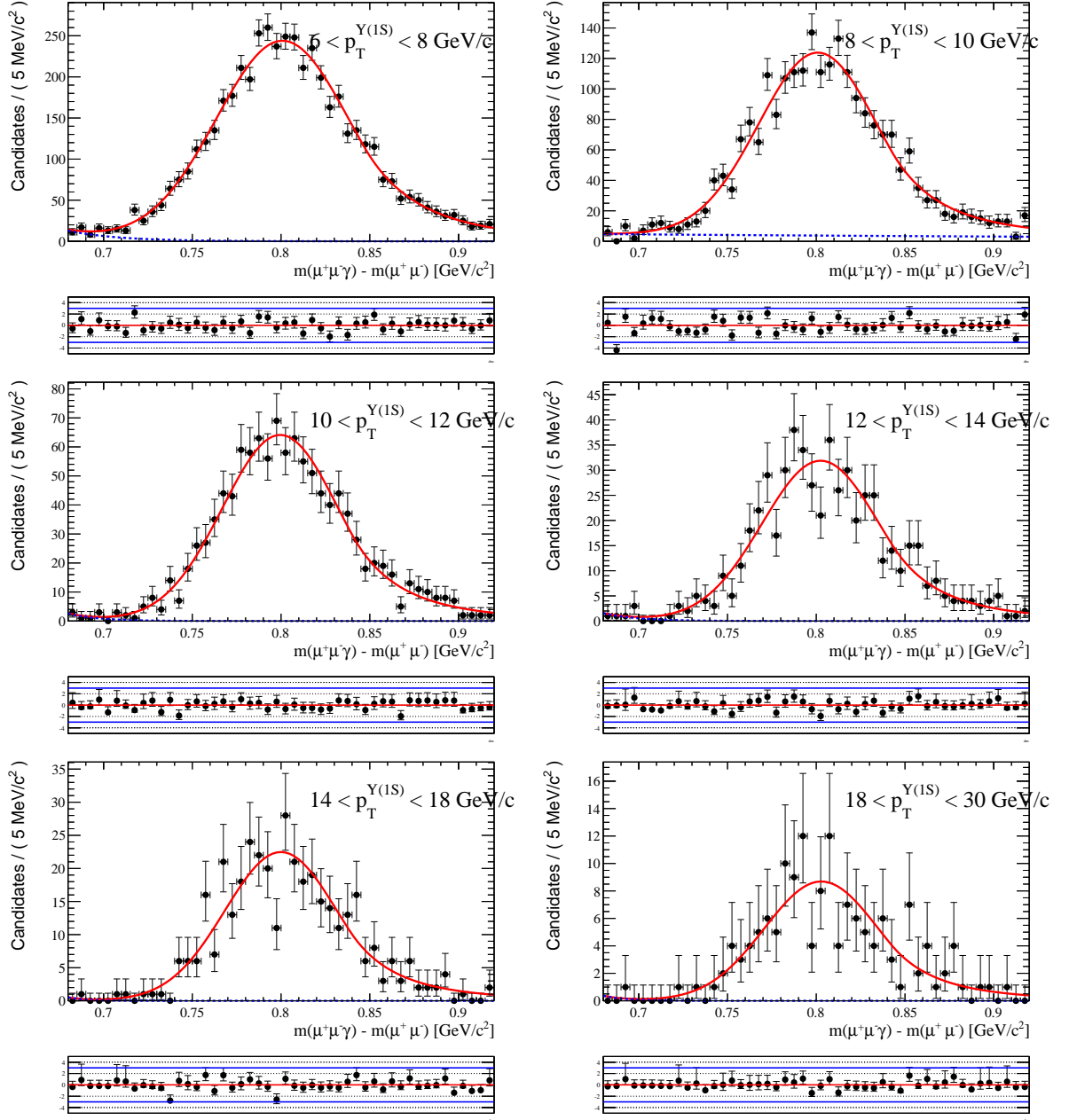


Figure 7:  $\chi_{b2}(2P)$

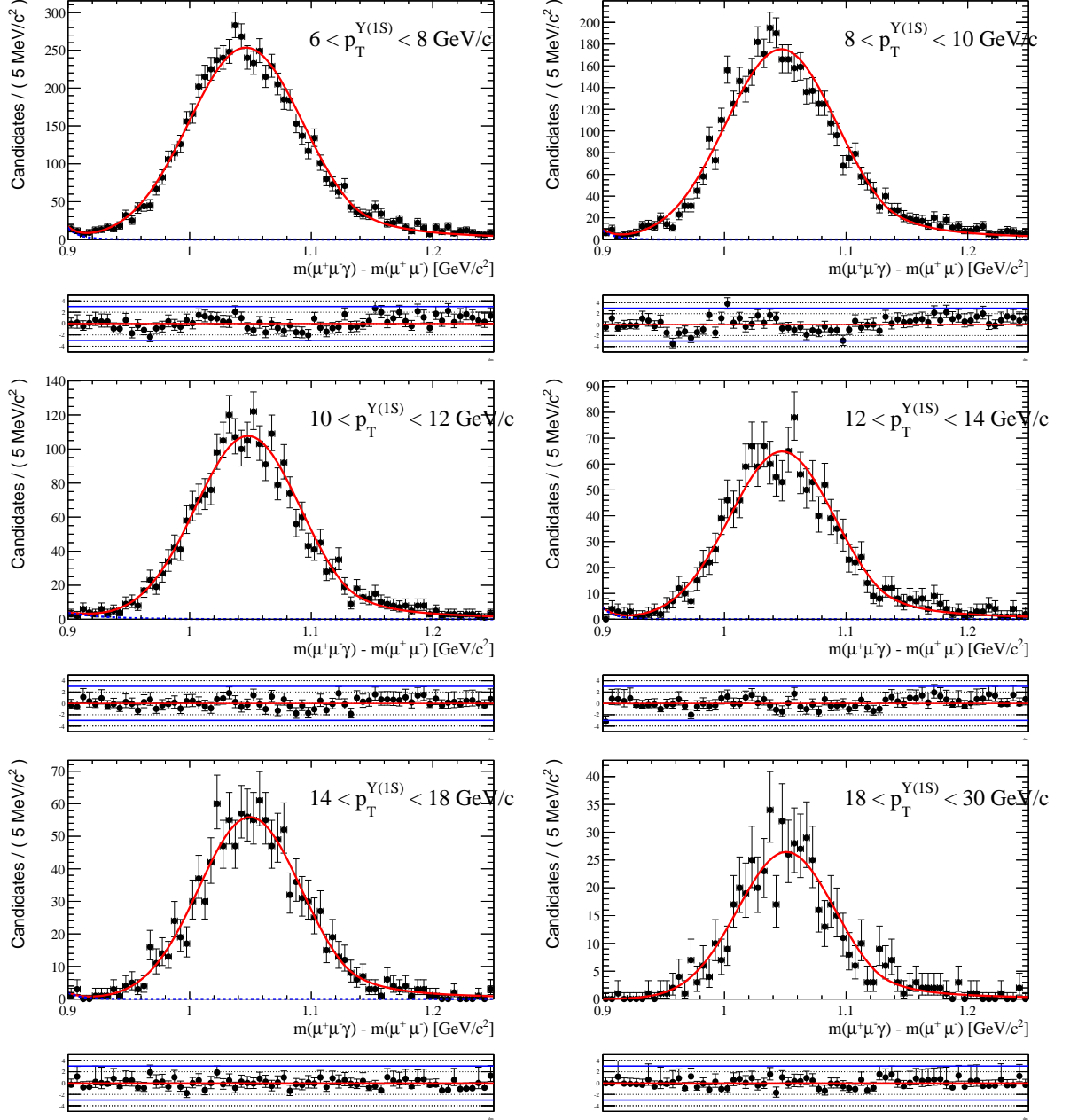


Figure 8: ( $\chi_{b1}3P$ )

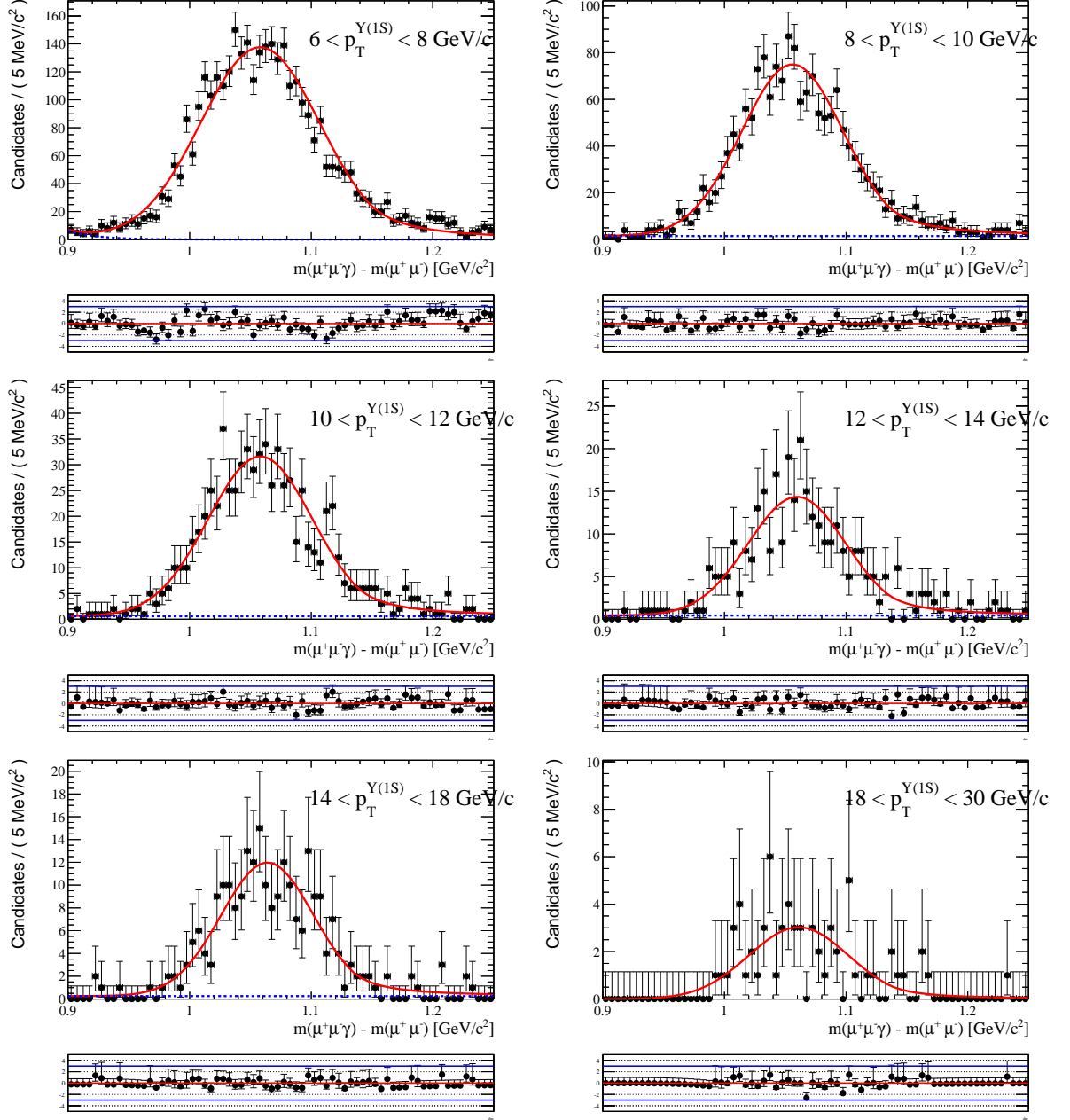


Figure 9:  $\chi_{b2}(3P)$